Brief communication: Soil moisture observations reconcile the discrepancy in detecting tornado early-stage track during the 24-25 March 2023 Mississippi outbreak

Jingyu Wang[1], Xianfeng Wang[2,3], Edward Park[1,2] and Yun Lin[4]

[1]National Institute of Education, Nanyang Technological University, Singapore 637616, Singapore
[2]Earth Observatory of Singapore, Nanyang Technological University, Singapore 639798, Singapore
[3]Asian School of the Environment, Nanyang Technological University, Singapore 639798, Singapore
[4]Joint Institute for Regional Earth System Science and Engineering, Department of Atmospheric and Oceanic Sciences, University of California, Los Angeles, Los Angeles, CA 722805, USA

Correspondence to: Jingyu Wang (jingyu.wang@nie.edu.sg) and Xianfeng Wang (xianfeng.wang@ntu.edu.sg)

Abstract. A series of tornadoes hit Western Mississippi on 24-25 March 2023, resulting in at least 26 deaths and massive destruction. The most devasting long-track EF4 tornado has been confirmed to touch down at southeast of Mayersville, Mississippi, however considerable inconsistency was found regarding its touchdown location and precise damage track between the onsite spotter reports and aftermath damage survey assessments. Such variation is a combined result of nocturnal occurrence (low nighttime visibility for spotter) and lack of assessment reference on non-vegetated farmland (high uncertainty of damage location for ground survey). This study suggests such discrepancy can be reconciled through the tornado damage scar captured by soil moisture observations.

1 Introduction

Tornadoes are one of the most devastating natural hazards that bring tremendous property damage, causalities, and economic loss to the United States (Changnon, 2009). The accurate detection of tornado track is essential for assessing the intensity, path, extent, touchdown location, and evolution of tornadoes. These data provide accurate ground-truth observations, enabling the quantitative evaluation of tornado simulations in numerical models. By doing so, it allows researchers to delve into the underlying processes that might not be captured by traditional measurements, improve the mechanism understanding and simulation, eventually promote the prediction skills for future events (Fan et al., 2023).

There are four types of tornado track detection methods, namely meteorological data analyses, witness report, ground survey, and remote sensing techniques. By monitoring the radar observation of key tornado indicators including the hook echo, rear flank downdraft, debris signature, and tornado-vortex related doppler velocity pattern (Bluestein, 2005), the presence of a tornado can be confirmed, thus its location and track can be estimated. However, this method relies on indirect measurements 'in the air' and may have difficulty accurately determining the exact location and path of a tornado. Human eyewitness of tornado and interpretation of misaligned landscapes used to be the best tornado detection system (Anderson et

al., 2007), but its accuracy is subject to human errors related to visibility, population distribution, and varying observation skills. Ground survey is conducted after the passage of tornadoes to assess the damage caused and determine the path of tornados. Various evidence is collected and examined, including the degree of structure damage, vegetation impact, and ground scouring patterns to estimate the strength and pathway of tornadoes (Doswell et al., 2009). The ground survey is further aided by remote sensing techniques. By comparing the aerial or satellite imagery pair taken before and after a tornado event, the damage track can be revealed by changes in land cover, such as the removal of vegetation, alteration of ground features, or the creation of new debris fields (Jedlovec et al., 2006).

Compared with the meteorological detection and eyewitness report that only provides the rough estimate of tornado location based on real-time observations, the aftermath ground survey and remote sensing techniques are most direct reflection of tornado passage, as ground texture has been severely perturbed, leaving damage scars on ground surface that can be quantitatively measured and assessed. However, the damage assessment methods heavily rely on the inspection of alterations in reference objects (e.g., affected building structure, uprooted trees, snaped trunks and power poles, and the destructed vegetation), which work best in regions well distributed with distinct features as well as the vegetated land surface. The rationale of the commonly used remote sensing-based damage track detection is, tornadoes disrupt the vegetation canopy, exposing the soil background, which exhibits contrasting reflective patterns in visible and near infrared channels (Cohen & Goward, 2004).

Over sparsely populated and non-vegetated areas like harvested farmland during the 24-25 March 2023 Mississippi nocturnal tornado outbreak (first report at 19:57 local time), all the primary approaches of conventional tornado track detection are facing significant challenge. First, the nighttime low visibility brings large uncertainty to storm spotters. Meanwhile, the low density of infrastructures and notable land features leaves the damage survey limited points of reference. Lastly, the bare surface voids the advantage of vegetation-based remote sensing.

To tackle the challenges of tornado track detection over less populated agricultural land without vegetation coverage, a recent study by the authors (Wang et al., 2023) showcased an application of using Moderate Resolution Imaging Spectroradiometer (MODIS; spatial resolution of 500 m) data at shortwave infrared (SWIR) channels to reconstruct tornado damage tracks. The algorithm is based on the understanding that when a tornado passes, the topmost dry soil layer is stripped away, exposing an underlying soil layer with a higher moisture content to the air, which results in significant signals on MODIS SWIR channels. Validated during the deadly 10–11 December 2021 tornado outbreak over northeastern Arkansas, this approach is thus a valuable substitute to the conventional vegetation-based tornado damage track detection (Kingfield and de Beurs, 2017; Bell and Molthan, 2016; Szwagrzyk et al., 2017) over non-vegetated winter farmland.

In this follow-up study, the same method is employed to analyze the 24-25 March 2023 Mississippi tornado outbreak, which occurred under similar conditions as the 2011 event, i.e., on non-vegetated farmland with the soil type of clayey vertisols in the Mississippi Alluvial Plain. Alongside the utilization of MODIS data, higher resolution satellite imagery is also adopted. Not only does this approach successfully confirm the tornado tracks identified by conventional methods, but it also exhibits the potential to reconcile discrepancies between human witness reports and ground survey of damage.

2 Data and Methods

MODIS serves as a pivotal instrument onboard the Terra and Aqua satellites, whose rapid daily update cycle and minimal data latency of a few hours makes it highly suitable for fast assessment of changes in land, cloud, aerosol properties. Although relatively coarse in spatial resolution (250–1000 m), MODIS has been proven capable of detecting tornado damage tracks based on reflectance differences at visible channels (Molthan et al., 2011), composed vegetation indices (Molthan et al., 2014), and soil moisture indices (Wang et al., 2023; hereafter 'WANG23'), as long as the path lengths are longer than its pixel size.

Soil moisture indices were generated using the MODIS channels 6 (1,628–1,652 nm) and 7 (2,105–2,155 nm) on two consecutive cloud-free days before (15 March 2023) and after (25 March 2023) the event, following the WANG23 method. To avoid redundancy, only the normalized shortwave-infrared difference soil moisture index 1 (NSDSI1) was shown. In addition to the MODIS data at 500 m resolution, various satellite imageries with higher resolution were also examined for more precise observation. Limited by their infrequent revisit and unfortunate coincidence with cloud contamination, finally the MultiSpectral Instrument (MSI) data obtained by Sentinel-2 was selected for the zoom-in view of soil moisture observation. Launched in June 2015 and March 2017 as twin satellites, Sentinel-2A and 2B carry the identical MSI (Phiri et al., 2020), whose channels 11 (1613.7 / 1610.4 nm) and 12 (2202.4 / 2185.7 nm) are equivalent to MODIS's SWIR channels, but with significantly higher resolution (20 m). It is importantly to note that unlike MODIS's comparison of 'before vs. after' the event, Sentinel-2's data are available after the event (26 March 2023) and a considerable time later (30 April 2023). As a result, the comparison of Sentinel-2's data was conducted as "after vs. recovery."

3 Results and Discussion

3.1 Examination of MODIS imagery

Based on the visual screening of MODIS image pair before (Fig. 1a) and after (Fig. 1b) the event over the domain of interest (30°N – 35°N, 87°W – 93°W). no significant linear patterns indicative of tornado damage tracks were detected. As shown in Fig. 1c, positive biases in NSDSI1 were observed over majority of the domain, indicating an overall increase in soil moisture. It is important to note that the average daily precipitation between the two available MODIS imageries is 8.6 mm/day (16-24 March, recorded at Rolling Fork, MS) with the maximum of 43.9 mm/day on 17 March. As a result, when picking up the pixels with the most significant increase in NSDSI1 as shown in Fig. 1d, the spatial coverage of such strong positive anomalies is considerably larger compared to what was reported in Fig. 1c and d of WANG23 for the December 2021 event, when the rainfall was weaker at 5.5 mm/day (recorded at Osceola, AR) between post-event (12 December) and pre-event (8 December).

As a result, although collocation between the pixels with significant positive bias in NSDSI1 and filtered tornado reports from National Oceanic and Atmospheric Administration (NOAA) Storm Prediction Center (SPC) is observed in Fig. 1d, it

remains challenging to precisely identify the tornado track based on MODIS imagery with moderate resolution. This difficulty arises due to the presence of numerous observations to the north of the identified tornado reports, which can be

100   attributed to the surface ponding effect resulting from excessive precipitation. Such large-scale homogeneous increase in soil moisture overwhelms the signals caused by tornadoes' suction removal of the topmost dry soil layer.

In contrast, as shown in Fig. 1e and f using the normalized difference vegetation index (NDVI; Rouse et al., 1974; defined as [NIR − red]/[NIR + red), the conventional vegetation-based damage detection method did not capture any anomalies indicative of tornado tracks.

105   It is evident that for the 24-25 March 2023 event, MODIS imagery is no longer suitable for the soil moisture-based tornado damage track detection. This is due to severe precipitation occurring between the available imageries, leading to overwhelming noise that greatly hampers the application of the WANG23 method. Additionally, the limited spatial resolution of MODIS can also impact the accuracy of the analysis. Consequently, higher-resolution Sentinel-2 imagery was utilized, employing the same soil moisture index. The analysis primarily focused on the reported initial touchdown location,

110   which is believed to strongly influence its progression to the EF4 level in later stage, but have the highest level of uncertainty due to its relatively weak severity at early stage.
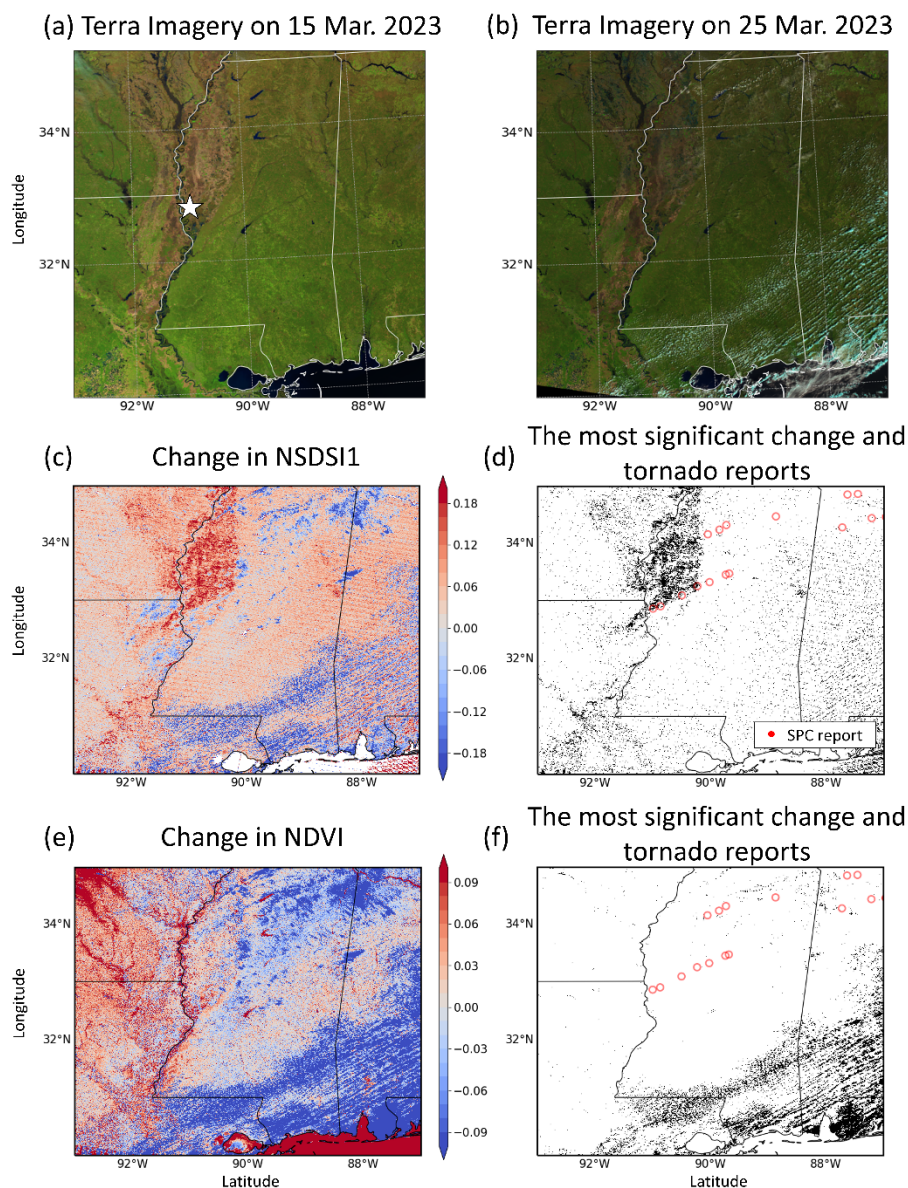
Figure 1: Natural color imagery captured by MODIS onboard the Terra satellite on (a) 16:15 UTC, 15 March 2023

115 **and (b) 16:30 UTC, 25 March 2023. (c) Change in normalized shortwave-infrared difference soil moisture index 1 (NSDSI1) (25 March minus 15 March). (d) Pixels with the most significant change (above 95th percentile) are marked with black dots. (e) and (f) are same as (c) and (d) but for Normalized Difference Vegetation Index (NDVI) with significance below 5th percentile. (d) and (f) are overlaid by the filtered tornado reports (red dots) obtained from National Oceanic and Atmospheric Administration (NOAA) Storm Prediction Center (SPC) archive. The white star**

120 **on (a) indicates the initial touchdown location where the high-resolution Sentinel-2 imagery is analyzed.**

3.2 Examination of Sentinel-2 imagery

By zooming into the initial touchdown region annotated in Fig. 1a (32.838°N – 32.853°N, 90.985°W – 91.005°W), Sentinel-2 imagery pair is compared between post-event (Fig. 2a) and one-month recovery (Fig. 2b) in natural color combination
125 (RGB). To facilitate visual interpretation, both images were enhanced by stretching their digital number value range from 0-255 scale to 0-50 scale. Some significant differences are observed between the two snapshots, namely the brighter patches to the northwest and the southeast of the domain, as well as a linear pattern between the two patches as indicated by yellow arrows in Fig. 2c. By overlaying the tornado damage track (red line) obtained from ground survey-based NOAA Damage Assessment Toolkit (DAT; https://apps.dat.noaa.gov/stormdamage/damageviewer/), the linear pattern seems indicative of the
130 tornado scar, however with considerable mismatch in precise location.

According to the classification map of the post-event imagery as shown in Fig. 2d, majority of the initial DAT tornado path occurred over non-vegetated land, suggesting the possibility of applying the WANG23 method to identify early tornado track. By subtracting 30 April from 26 March, Fig. 2e illustrates the change in NSDSI1 caused by tornado passage. Negative biases prevail the entire domain except for a few pixels that exhibit surplus soil moisture. These pixels with higher soil
135 moisture are not collocated with either SPC or DAT point-based report, but they appear to align with the lines connecting those reports.

To facilitate a clear comparison, Fig. 2f isolates the pixels with the most significant positive bias (black dots) using the same method as Fig. 1d. Their spatial distribution is then overlaid with the DAT damage track (red line) and damage area (green polygon), as well as the estimated SPC track (purple line). Note the SPC data are point-based reports, therefore the SPC
140 track is made by connecting the earliest report (32.84°N, 91°W) with the subsequent report (32.91°N, 90.87°W).

There are three conspicuous clusters of black dots exhibiting a noteworthy linear pattern, which are labelled as C1, C2, and C3. C1 is well aligned with the DAT track, whereas C2 and C3 are precisely positioned along the SPC track. The correlation observed between notably disrupted NSDSI1 signals and the tornado tracks detected by different methods provides additional validation for the robustness of the WANG23 method. The soil moisture-based approach exhibited much
145 improved accuracy when utilizing higher resolution images as opposed to MODIS.

There is a potential concern that comparing post-event with one-month recovery could introduce even greater uncertainty. This is because both meteorological factors (e.g., gusty winds, strong precipitation, hail, and additional tornadoes) and non-meteorological factors (e.g., agricultural activities) could contribute to further perturbation of the land surface. However, based on records from DAT and meteorological observations, no hazardous weather events occurred in the region from 27
150 March to 30 April. Additionally, an average precipitation rate of 4.4 mm/day was reported during this period, which aided in the recovery of the affected land surface from tornado damage (Fig. 2b). As for agricultural activities, the next planting season did not commence until early May. As a result, apart from utilizing high-resolution imagery, the 'after vs. recovery'

comparison performed in this study provides a fresh perspective for satellite-based detection of tornado damage tracks, particularly when unfavorable meteorological conditions make the traditional "before vs. after" comparison infeasible.
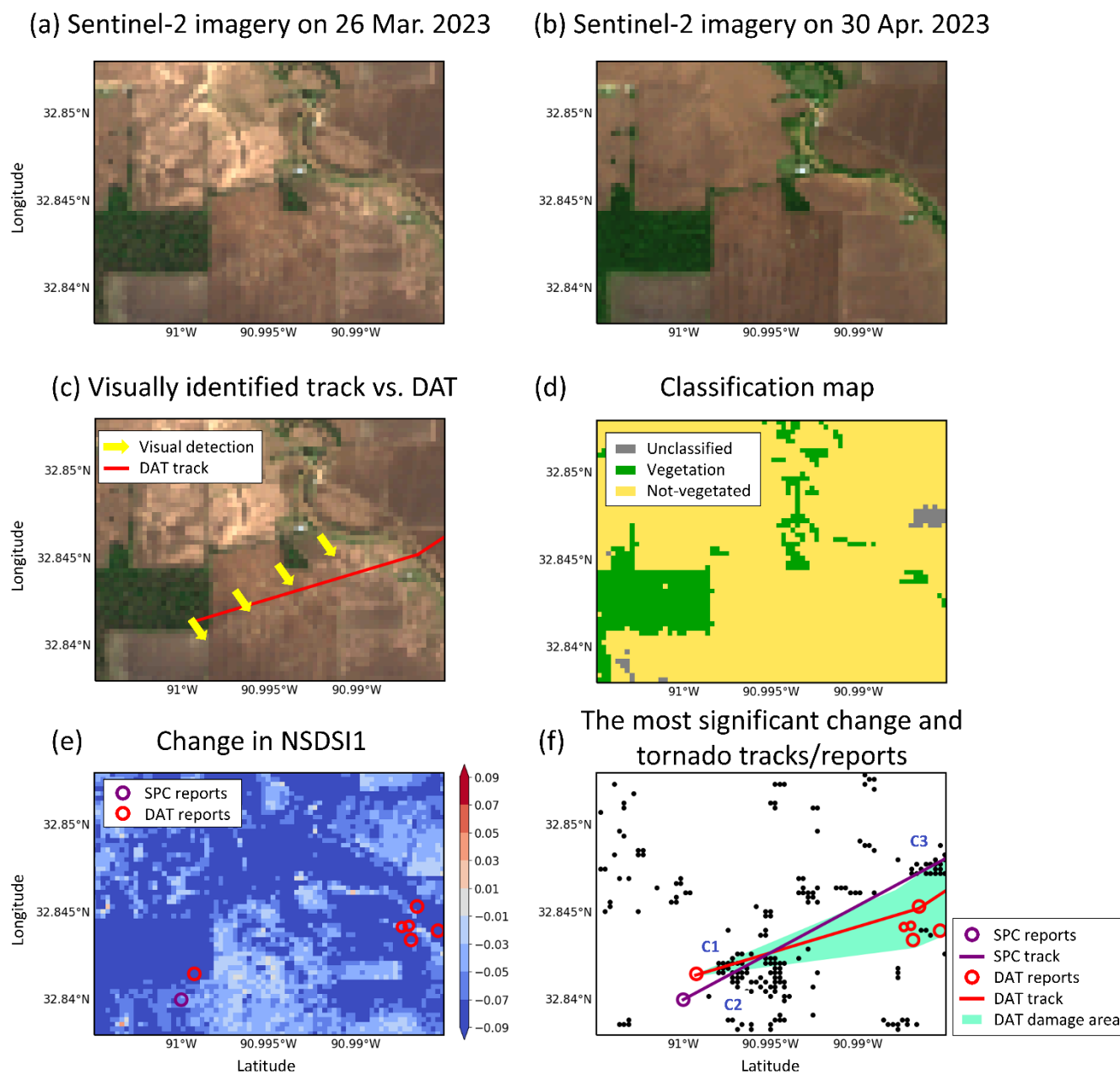
Figure 2: Natural color imagery captured by Sentinel-2 on (a) 26 March 2023 (post-event) and (b) 30 April 2023 (one-month recovery). (c) is same as (a) but overlaid by tornado tracks obtained from NOAA DAT survey (red line) and visual identification (yellow arrows). (d) The classification map based on (a). (e) Change in NSDSI1 (26 March minus

30 April). Pixels in (e) with the most significant change (above 95th percentile) are marked with black dots in (f),
160   **overlaid by the first SPC tornado report (purple circle) and the line (purple line) connecting the first two SPC**
reports, as well as the DAT damage reports (red circles), damage track (red line), and damage area (green polygon).

3.3 Implication to reconciling the discrepancy in different tornado damage track detection methods

None of the existing tornado damage detection method is perfect. SPC's storm spotter report is associated with large
uncertainties, particularly with low visibility during nighttime. DAT's ground survey heavily relies on the damage
165   assessment. Unfortunately, both limitation (i.e., nocturnal occurrence and lack of assessment reference) were encountered
during the 24-25 March tornado touchdown.

Upon closely comparing the tornado tracks identified by the two distinct methods as illustrated in Figure 2f, it appears that
the SPC track exhibits better alignment with the visible scar highlighted in Figure 2c. Conversely, while the initial DAT
tornado report is in proximity to the SPC's report, the DAT track veers in a clockwise direction compared to the SPC track
170   and extends further towards the south. The discrepancy in the DAT track may be attributed to the magnetic effect of the
damage point located at 32.845°N, 90.987°W. The detailed report describes "several trunks snapped with clear convergence
in tree fall here" at that location. However, as depicted in Fig. 2d, this specific location is the only place with vegetation
coverage, therefore its reliability as an indicator of tornado passage is questionable. Additionally, unlike strong signals such
as uprooted trees, snapped trunks can also be caused by derechos or gusty winds in close vicinity to the tornado, which
175   introduces an additional layer of uncertainty to the DAT track.

In such situations, additional evidence is necessary to confirm the exact tornado damage track, which can be obtained
through the analysis of perturbed soil moisture. No pixels exhibiting a significant surplus in NSDSI1 are found in the
proximity of this questionable DAT report. However, the clusters of NSDSI1 surplus labelled as C1, C2, and C3 align well
with both the SPC track and the initial portion of the DAT track. As a result, this particular DAT report could be influenced
180   by the absence of assessment reference, which eventually pulls the DAT track towards it.

4 Conclusions

Building upon the findings in a preceding study by the authors (Wang et al., 2023), this brief communication successfully
applied the soil moisture-based tornado damage track detection method to the 24-25 March 2023 Mississippi outbreak. In
addition to a case validation of the established method using higher-resolution satellite imagery, as well as testing the 'after
185   vs. recovery' comparison instead of 'before vs. after' comparison, this study also found that the notable discrepancies
between spotter reports and ground survey assessments at the tornado early stage can be reconciled using the new method.

The observed inconsistency between the two conventional tornado track detection method was primarily attributed to the
nocturnal occurrence (uncertainty in spotter reports) and the lack of reference on non-vegetated farmland (uncertainty in
damage assessment). However, these limitations cannot impact soil moisture observation. Using the WANG23 method, both

190 the SPC track and the initial portion of the DAT track were well confirmed. Most importantly, a possible biased DAT report was recognized because of its exclusive reliance on vegetation coverage without the support of the collocated soil moisture evidence.

In summary, by using a case study of the 24-25 March 2023 Mississippi outbreak, this study has validated the effectiveness of a recently developed tornado damage track detection method based on soil moisture. By utilizing SWIR channels as
195 detailed in WANG23, this method has been proven most suitable for tornado events in sparsely populated, unvegetated farmland. The results from WANG23 and this study demonstrated that this method has the potential to serve as a valuable auxiliary complement to conventional detection methods. Moreover, the utilization of SWIR channels has shown significant advantages in capturing subtle land surface scars compared to visible channels, as evident from the comparison of visible imagery pair in Fig. 2a and b. Specifically, Fig. 2a showed widespread storm-induced perturbation in the northwest region
200 relative to Fig. 2b. However, those disturbances were too superficial to leave soil moisture scars in Fig. 2f, indicating the superior performance of SWIR channels in reducing the signal-to-noise ratio compared to visible channels. Therefore, incorporating SWIR channels in future remote sensing-based damage track detection applications, including aerial platforms, satellites, and unmanned aerial systems, is highly recommended.

Competing Interests

205 The contact author has declared that none of the authors has any competing interests.

Acknowledgments

This research is supported by the National Institute of Education, Singapore, under its Academic Research Fund (RI 5/22 WJY), Academic Research Fund Tier 2 (MOE-T2EP402A20-0001 to E. P.) and (MOE2019-T2-1-174 (S) to X. W.). Any opinions, findings and conclusions or recommendations expressed in this material are those of the authors and do not reflect
210 the views of the National Institute of Education, Singapore.

References

Anderson, C. J., Wikle C. K. , Zhou Q. , and Royle J. A.: Population influences on tornado reports in the United States. Wea. Forecasting, 22, 571–579, https://doi.org/10.1175/WAF997.1, 2007.

Bell, J. R. and Molthan, A. L.: Evaluation of approaches to identifying hail damage to crop vegetation using satellite
215 imagery. Journal of Operational Meteorology, 4(11), 142– 159. https://doi.org/10.15191/nwajom.2016.0411, 2016.

Bluestein, H. B.: A review of ground-based, mobile, W-band Doppler-radar observations of tornadoes and dust devils. Dyn. Atmos. Oceans, 40, 163–188, 2005.

Changnon, S. A.: Tornado losses in the United States. Natural Hazards Review, 10(4), 145– 150. https://doi.org/10.1061/(ASCE)1527-6988(2009)10:4(145), 2009.

220 Cohen, W. B., and Goward, S. N.: Landsat's role in ecological applications of remote sensing. BioScience, 54(6), 535–545. https://doi.org/10.1641/0006-3568(2004)054[0535:lrieao]2.0.co;2, 2004.

Doswell, C. A. III, H. E. Brooks, and N. Dotzek, N.: On the implementation of the enhanced Fujita scale in the USA. Atmos. Res. ,93, 554–563, https://doi.org/10.1016/j.atmosres.2008.11.003, 2009.

Fan, J., Wang, J, and Lin, Y.: Urbanization may enhance tornado potential: A single case report. Front. Earth Sci., 11, 225 https://doi.org/10.3389/feart.2023.1148506, 2023.

Jedlovec, G. J., Nair, U., and Haines, S. L.: Detection of storm damage tracks with EOS data. Weather and Forecasting, 21(3), 249–267. https://doi.org/10.1175/waf923.1, 2006.

Kingfield, D. M. and de Beurs, K. M.: Landsat identification of tornado damage by land cover and an evaluation of damage recovery in forests. Journal of Applied Meteorology and Climatology, 56(4), 965– 987. https://doi.org/10.1175/JAMC-D-16- 230 0228.1, 2017.

Molthan, A. L., Bell, J. R., Cole, T. A., and Burks, J. E.: Satellite-based identification of tornado damage tracks from the 27 April 2011 severe weather outbreak. Journal of Operational Meteorology, 2(16), 191– 208. https://doi.org/10.15191/nwajom.2014.0216, 2014.

Molthan, A., Jedlovec, G., and Carcione, B.: NASA satellite data assist in tornado damage assessments. Eos, Transactions 235 American Geophysical Union, 92(40), 337– 339. https://doi.org/10.1029/2011eo400002, 2011.

Phiri D., Simwanda M., Salekin S., Nyirenda V. R., Murayama Y. and Ranagalage M.: Sentinel-2 Data for Land Cover/Use Mapping: A Review. Remote Sensing. 2020; 12(14):2291. https://doi.org/10.3390/rs12142291, 2020.

Szwagrzyk, J., Gazda, A., Doborwolska, D., Checko, E., Zaremba, J., and Tomski, A.: Tree mortality after wind disturbance differs among tree species more than among habitat types in a lowland forest in northeastern Poland. Forest Ecology and 240 Management, 398, 174– 184. https://doi.org/10.1016/j.foreco.2017.04.041, 2017.

Wang, J., Lin, Y., McFarquhar, G. M., Park, E., Gu, Y., Su, Q., et al.: Soil moisture observations from shortwave infrared channels reveal tornado tracks: A case in 10–11 December 2021 tornado outbreak. Geophysical Research Letters, 50, e2023GL102984. https://doi.org/10.1029/2023GL102984, 2023.